2/7/2012 4:22:41 PM **RAPID**

University of Kansas **KKU**
In Process Date:

ILL Number: -5168138

Odyssey: **206.107.44.64**

Ariel:
129.82.28.195

Email:

Maxcost:

KKU Billing: **Exempt**

Paging notes:
___Call # NOS ___Call #≠ Title
Book/Volume/Issue/Series NOS (Circle)
Year _____ ≠ Volume _____
___Article not found as cited – Why?_____
___
Initials_____

Staff notes:
OCLC#: 9705204
ISSN#: 0171-9335

Lending String:

Lending Articles

Call #:
http://rapidill.org/redir.ashx?id=MzQ3NzcyMTE=

Location: **ScienceDirect**

Journal Title: **European journal of cell biology**

Volume: **90** Issue: **10**

Month/Year: **2011**

Pages: **825-833**

Article Author:

Article Title: **Pil1, an eisosome organizer, plays an important role in the recruitment of synaptojanins and amphiphysins to facilitate receptor-mediated endocytosis in yeast**

ILLiad TN: 1273096

Borrower: RAPID:AFU

Shipping Address:
NEW: Main Library
Rapid

European Journal of Cell Biology 90 (2011) 825–833

Contents lists available at ScienceDirect

European Journal of Cell Biology

journal homepage: www.elsevier.de/ejcb

Pil1, an eisosome organizer, plays an important role in the recruitment of synaptojanins and amphiphysins to facilitate receptor-mediated endocytosis in yeast

Erin R. Murphy, Jacob Boxberger, Robert Colvin, Suk Je Lee, Geoffrey Zahn, Fred Loor, Kyoungtae Kim*

Department of Biology, Missouri State University, 901 South National Ave., Springfield, MO 65897, USA

ARTICLE INFO

Article history:
Received 28 March 2011
Received in revised form 25 May 2011
Accepted 11 June 2011

Keywords:
Eisosome
Pil1
Synaptojanin
Amphiphysin
Receptor-mediated endocytosis
Yeast

ABSTRACT

The eisosome protein Pil1 is known to be implicated in the endocytosis of Ste3, but the precise biological function of it during endocytosis is poorly understood. Here, we present data to reveal Pil1's role in receptor-mediated endocytosis. Using live cell imaging, we show that endocytic patches carrying Abp1 and Las17 persisted much longer in *PIL1*-deficient cells. The loss of Pil1 also greatly affected both the scission efficiency and the frequency of formation of endocytic sites carrying Rvs161- and Rvs167-GFP. Furthermore, the mistargeting of the synaptojanins, Sjl1 and Sjl2, to the cytoplasm in *pil1*Δ cells suggests that Pil1 is required for the proper recruitment of the synaptojanins to endocytic sites. A severe motility defect of Abp1-GFP during its internalization in a codeletant of *PIL1* and *SJL2* indicates a functional interplay between them in endocytosis. Together, these results establish that Pil1 is involved in the recruitment of endocytic proteins to optimize endocytosis.

Published by Elsevier GmbH.

Introduction

Endocytosis is the process in which the plasma membrane invaginates to take up essential nutrients, lipids, and surface receptors. At the molecular level, the mechanism by which endocytosis initiates at particular sites on the plasma membrane is poorly understood. However, previous studies have suggested that large immobile protein assemblies called eisosomes not only mark the site of endocytosis but also ensure an even distribution of potential endocytic sites (Moreira et al., 2009; Walther et al., 2006). It appears that Pil1 plays a more important role than other components of the eisosome in maintaining the structural integrity of it since loss of Pil1 leads to a severe disruption of eisosome organization (Grossmann et al., 2007; Walther et al., 2006). Two functionally redundant serine/threonine protein kinases Pkh1/2, which physically associate with the eisosome, have been shown to phosphorylate Pil1 *in vitro*, and perturbation of Pil1 phosphorylation affects Pil1 assembly into eisosomes (Walther et al., 2007; Zhang et al., 2004): the dephosphorylated form of Pil1 preferentially assembles into eisosomes, and hyperphosphorylation of Pil1 causes its disassembly from eisosomes. Besides Pil1 and Pkh1/2, many more genes (88) appear to be involved in the organization of the eisosome according to a genome-wide screen for genes affecting eisosomes (Frohlich et al., 2009).

Membrane invagination and its subsequent pinch-off event are followed by spatiotemporal recruitment of endocytic proteins. Once an endocytic site is selected, actin-independent endocytic proteins, such as clathrin, Las17, and Pan1, are recruited to the site (Jonsdottir and Li, 2004; Kaksonen et al., 2003, 2005; Newpher et al., 2005). Actin and actin binding proteins, including Abp1 and Arp2/3 complex, then arrive at the site, and initiate rapid polymerization of actin that drives the formation of the invaginated membrane (Merrifield et al., 2004). Membrane fission must then occur to release an endocytic vesicle, perhaps by a rapid burst of actin polymerization and the membrane tubulating activity of the amphiphysins, Rvs161 and Rvs167 (Galletta and Cooper, 2009; Kaksonen et al., 2005; Youn et al., 2010).

A recent yeast endocytic fission model emphasizes the role of the amphiphysins for proper scission (Liu et al., 2009): based on the finding by a previous EM study that Rvs167 localizes at the intermediate area (or neck) of invaginated pits (Idrissi et al., 2008), Liu et al. (2009) proposed that the amphiphysins bind to the membrane curvature at the neck and protect the underlying PIP_2 from hydrolysis mediated by the access of the synaptojanins, Sjl1 and Sjl2. In contrast, they predicted that depletion of PIP_2 occurs rapidly at the tip of the invagination due to the full access of the synaptojanins. The unequal levels of PIP_2 across the endocytic invagination appear to generate an interfacial force which squeezes the bud neck and as a result vesicle scission occurs.

* Corresponding author. Tel.: +1 417 836 5440, fax: +1 417 836 5126.
E-mail address: kkim@missouristate.edu (K. Kim).

0171-9335/$ – see front matter. Published by Elsevier GmbH.
doi:10.1016/j.ejcb.2011.06.006

Although previous evidence has suggested that Pil1 is implicated in yeast endocytosis (Walther et al., 2006), the precise function of it during the endocytic process remains undiscovered. In this study, we provide evidence that Pil1 functions in proper recruitment of the synaptojanins and the amphiphysins to endocytic sites, required for efficient receptor-mediated endocytosis. Importantly, we show that the deletion of *SJL2* in the background of *pil1*Δ further perturbs endocytosis, most likely due to the disruption in the actin cytoskeleton.

Methods and materials

Yeast strain construction and media

Yeast strains used in this study are listed in Table 1. Strains expressing GFP- or RFP-fused proteins were constructed by integrating respective GFP or RFP sequence at the 3′end of the gene of interest as described previously (Kim et al., 2006; Longtine et al., 1998; Nannapaneni et al., 2010). Cells expressing both GFP- and RFP-fused proteins were constructed by the same method. To generate gene deletion mutants, WT cells were transformed with PCR product carrying a disruption construct as described before (Longtine et al., 1998). Double deletion mutant strains (*pil1*Δ*sjl2*Δ, *pil1*Δ*rvs161*Δ, and *pil1*Δ*rvs167*Δ) were prepared by crossing various strains of haploid *pil1*Δ cells with *sjl2*Δ, *rvs161*Δ, or *rvs167*Δ, followed by dissecting haploid seeds and by screening the genotypes of them. One deletion strain (*sjl2*Δ) was obtained from Scott Emr's lab. All yeast strains were grown in standard yeast peptone dextrose (YPD) medium and cultured at 30 °C, unless otherwise stated.

Spinning confocal microscopy

Time-lapse movies and still images of GFP or RFP labeled cells were made with a spinning disk confocal system that includes an inverted Olympus IX81 microscope, a Yokogawa CSUX1 spinning disk head, a 100× numerical aperture (NA) 1.4 PlanApo oil objective, and an Electron Amplified CCD (ImagEM, Hamamatsu). The temperature of the specimen and stage was maintained at 30 °C. The image was focused at an equatorial plane of the cells. For time-lapse movies of GFP- or RFP-fused proteins, a single channel was utilized, and movies were captured at 2 frames/s for movie duration of 1 min. Simultaneous two-color imaging was done using an image splitter to separate red and green emission signals.

Measurement of patch lifetime at the membrane and kymograph

To examine patch lifetime at the membrane we used the following 3 independent microscopic analyses. First, the time spent by a GFP-fused protein at the membrane (from the time of its appearance to the time at which it moves away from its origin or disappears) was manually determined as described previously (Nannapaneni et al., 2010). For example, a total of 15–30 newly forming patches at the membrane were used to determine the mean membrane lifespan of Abp1-GFP patches. Patches that at any point in their lifetime are too close to another patch to be clearly resolved were excluded from our analysis. Second, to directly visualize the duration of time spent by a patch on the membrane, a kymographic representation of GFP- or RFP-fused proteins in a single patch over time was made using SlideBook (v.5). Third, the fluorescence intensity profile of endocytic patches over time was also made using SlideBook (v.5).

Computer-assisted tracking of patch movement

Time-lapse movies of GFP- or RFP-fused proteins in WT and *pil1*Δ cells were analyzed with the aid of a patch tracking software to quantitate the behavior and degree of patch motion. As described previously (Carlsson et al., 2002; Kim et al., 2006; Nannapaneni et al., 2010), the square of the patch displacement (μm^2) from the origin over time was determined. The mean squared displacement (MSD, μm^2) of Abp1-GFP patches was calculated by analyzing 15–30 newly forming patches at the cell cortex.

Actin staining with fluorescein isothiocyanate (FITC)-Phalloidin

Yeast actin cytoskeleton was stained with FITC-Phalloidin using the method described previously (Kamble et al., 2011). Cells were fixed by formaldehyde (5% final concentration) and sonicated briefly. F-actin was stained by 1 μl of a 3.3 μM stock of FITC-Phalloidin for 15 min in dark. Cells were visualized under the spinning confocal microscope equipped with Orca-R2 camera. To determine the percentage of actin polarization, fluorescence images were quantified by counting 50 cells from each strain. Cells were classified as polarized when fewer than 5 actin patches were present in the mother portion of small budded cells. In particular, to measure the amount of F-actin at the cortical patches, images were taken at the same exposure rate of 100 ms, followed by measuring the fluorescence intensity of the cortical patches using ImageJ software.

Cell growth assay

A spotting assay was performed to dilute cells by a factor of 5 onto YPD plates. The plates were then grown for 2 days at 30 °C or 37 °C. A liquid growth assay was performed to determine doubling time of cells.

Results

Loss of Pil1 affects receptor-mediated endocytosis

Consistent with the previous findings that Pil1 plays a role in endocytosis (Walther et al., 2006), we found a delay in the trafficking of FM4-64 dye, which follows liquid-phase endocytosis, to the vacuole in *pil1*Δ cells (Data not shown). In order to investigate whether Pil1 plays a role in receptor-mediated endocytosis (RME), we tagged two well-validated RME markers Las17 and Abp1 with GFP at their C-termini, and recorded time-lapse fluorescence images. Las17, an Arp2/3 complex activator, arrives at endocytic sites and stays immobile prior to its disassembly (Kaksonen et al., 2003). To characterize any effects caused by loss of Pil1 on the assembly dynamics of Las17-GFP, we measured the membrane lifespan of Las17-GFP in both WT and *pil1*Δ cells by calculating the time spent by Las17-GFP at the endocytic site. The mean membrane lifespan of Las17-GFP in WT cells (28.8 ± 3.4 s) was in agreement with that of previous studies (Kaksonen et al., 2003; Kim et al., 2006; Nannapaneni et al., 2010), whereas Las17-GFP in *pil1*Δ cells persisted much longer at its origin with the mean lifespan of 51.5 ± 17.3 s (Fig. 1A). Actin binding protein Abp1 is a well-characterized late marker of RME. It arrives at endocytic sites (hitherto, actin patch) approximately 5–8 s before pinch-off process, moves away from the site in a directed manner, and departs from the postinternalized actin patches to be reused for the next round of endocytosis (Kim et al., 2006; Toret et al., 2008). The membrane lifespan of Abp1-GFP (17.2 ± 3.2 s) in *pil1*Δ cells was about two times longer than in WT cells (8.2 ± 1.7 s) (Fig. 1B). As shown in Fig. 1C and D, our kymograph and fluorescence intensity profile

Table 1
Yeast strains used in this study.

Strain	Source	Genotype
KKY 0036	Invitrogen	*Mat α his3Δ leu2Δ lys2Δ ura3Δ, LAS17-GFP-HIS3*
KKY 0194	Invitrogen	*Mat α his3Δ leu2Δ lys2Δ ura3Δ, pil1Δ::KanMX6*
KKY 0197	Invitrogen	*Mat α his3Δ leu2Δ lys2Δ ura3Δ*
KKY 0343	Invitrogen	*Mat α his3Δ leu2Δ lys2Δ ura3Δ trp1Δ*
KKY 0397	This study	*Mat α his3Δ leu2Δ lys2Δ ura3Δ, ABP1-GFP-HIS3*
KKY 0399	This study	*Mat α his3Δ leu2Δ lys2Δ ura3Δ, pil1Δ::KanMX6, ABP1-GFP-HIS3*
KKY 0402	This study	*Mat α his3Δ leu2Δ lys2Δ ura3Δ, pil1Δ::KanMX6, LAS17-GFP-HIS3*
KKY 0421	Stefan et al. (2005)	*Mat a his3Δ leu2Δ lys2Δ ura3Δ trp1Δ suc2Δ, sjl2Δ::HIS3, sst1Δ::URA3*
KKY 0438	This study	*Mat α his3Δ leu2Δ lys2Δ ura3Δ, SJL2-GFP-HIS3*
KKY 0490	This study	*Mat a his3Δ leu2Δ ura3Δ ade3Δ trp1Δ, pil1Δ::KanMX6, sjl2Δ::HIS3*
KKY 0495	This study	*Mat a his3Δ leu2Δ met15Δ ura3Δ, rvs167Δ::KanMX6, ABP1-GPF-HIS3*
KKY 0528	This study	*Mat a his3Δ leu2Δ ura3Δ ade3Δ trp1Δ, pil1Δ::KanMX6, sjl2Δ::HIS3, ABP1-GFP-TRP1*
KKY 0531	This study	*Mat α his3Δ leu2Δ lys2Δ ura3Δ, pil1Δ::KanMX6, SJL2-GFP-HIS*
KKY 0570	This study	*Mat α his3Δ leu2Δ lys2Δ ura3Δ pil1Δ::KanMX6, SJL1-GFP-HIS3*
KKY 0571	This study	*Mat α his3Δ leu2Δ lys2Δ ura3Δ pil1Δ::KanMX6, SJL3-GFP-HIS3*
KKY 0610	This study	*Mat a his3Δ leu2Δ lys2Δ ura3Δ trp1Δ suc2Δ, sjl2Δ::HIS3, sst1Δ::URA3, ABP1-GFP-TRP1*
KKY 0617	This study	*Mat a his3Δ leu2Δ ura3Δ ade2Δ trp1Δ can1Δ, RVS161-GFP-HIS3*
KKY 0623	This study	*Mat α his3Δ leu2Δ lys2Δ ura3Δ, SJL3-GFP-HIS3*
KKY 0631	This study	*Mat α his3Δ leu2Δ lys2Δ ura3Δ, pil1Δ::KanMX6, RVS161-GFP-HIS3*
KKY 0659	This study	*Mat α his3Δ leu2Δ lys2Δ ura3Δ, SJL1-GFP-HIS3*
KKY 0653	This study	*Mat α his3Δ leu2Δ lys2Δ ura3Δ, pil1Δ::KanMX6, RVS167-GFP-HIS3*
KKY 0661	This study	*Mat α his3Δ leu2Δ lys2Δ ura3Δ, RVS167-GFP-HIS3*
KKY 0694	This study	*Mat α his3Δ leu2Δ met15Δ ura3Δ trp1Δ, pil1Δ::KanMX6, rvs161Δ::HIS3, ABP1-GFP-TRP1*
KKY 0709	This study	*Mat α his3Δ leu2Δ lys2Δ ura3Δ trp1Δ, pil1Δ::HIS3, RVS167-GFP-TRP1, ABP1-RFP-KanMX6*
KKY 0713	This study	*Mat a his3Δ leu2Δ lys2Δ ura3Δ trp1Δ, pil1Δ::KanMX6, rvs167Δ::HIS3, ABP1-GFP-TRP*
KKY 0715	This study	*Mat α his3Δ leu2Δ lys2Δ ura3Δ trp1Δ, pil1Δ::HIS3, RVS161-GFP-TRP1, ABP1-RFP-KanMX6*
KKY 0738	This study	*Mat α his3Δ leu2Δ lys2Δ ura3Δ trp1Δ, rvs161Δ::HIS3, ABP1-GFP-TRP1*
KKY 0744	This study	*Mat α his3Δ leu2Δ lys2Δ ura3Δ trp1Δ, RVS167-GFP-HIS3, ABP1-RFP-KanMX6*
KKY 0747	This study	*Mat α his3Δ leu2Δ lys2Δ ura3Δ trp1Δ, RVS161-GFP-HIS3, ABP1-RFP-KanMX6*

analysis over time confirmed the extended membrane lifespans of actin patches carrying Abp1- and Las17-GFP in *pil1*Δ cells.

Because most newly formed Abp1-GFP patches (~90%) in *pil1*Δ cells were internalized and moved away from the cell cortex after the observed prolonged lifespan, we examined the behavior and extent of patch motion during the entire lifespan of Abp1-GFP, from its appearance at the cell cortex to dissociation from the postinternalized patch, by determining the squared patch travel displacement (μm^2) from the site of origin with the aid of a particle tracking software (Nannapaneni et al., 2010). The mean squared displacement (MSD, μm^2) values of 30 Abp1-GFP patches from WT and *pil1*Δ cells were plotted against time (s) (Fig. 1E). Consistent with the membrane Abp1-GFP lifespan (Fig. 1B), MSD in WT cells increased negligibly for the first 7 s, indicative of patches being tethered to the cell cortex. The slope of MSD increases drastically when the patches move in a directed manner, showing a concave-up slope (Fig. 1E). In *pil1*Δ cells, the MSD curve showed an extended tethering time, followed by a concave-up slope, which was less steep than that of WT cells. This indicates that Abp1-GFP patches in *pil1*Δ cells stayed longer at and move away from their origin in a directed manner, albeit at a slower rate. Together, loss of Pil1 affects the receptor-mediated endocytosis by significantly extending the membrane lifespan of actin patch markers and by reducing Abp1-GFP patch motility.

*Amphiphysin and synaptojanin recruitment impaired in pil1*Δ *cells*

Since loss of Pil1 affects the dynamics of Abp1-GFP and Las17-GFP, we reasoned that deletion of *PIL1* may also affect the dynamics of other endocytic factors. A previous study showed that the yeast amphiphysin ortholog Rvs161 physically interacts with Pil1 (Krogan et al., 2006). We thus first tested the effect of deletion of *PIL1* on the dynamics of Rvs161 and its homolog Rvs167. Consistent with a previous finding (Kaksonen et al., 2005), Rvs161-GFP and Rvs167-GFP in WT cells localized to cortical patches and also to the cytoplasm, whereas in *PIL1*-deficient cells the cytoplasmic diffusion of the GFP-fused amphiphysins appeared to increase (Fig. 2A). Also, patches carrying GFP-fused amphiphysins showed a two-fold increase in membrane lifespan in *pil1*Δ cells, as depicted in our kymographic representations of Rvs161- and Rvs167-GFP (Fig. 2B). Noteworthy, the *PIL1* mutants showed a significant decrease in cortical Rvs161-GFP and Rvs167-GFP patch numbers. Our quantitative movie analysis revealed 81% and 74% decreases in the number of Rvs161-GFP and Rvs167-GFP patches, respectively, in the *pil1*Δ mutants (Fig. 2C). Consistently, a simultaneous two-color analysis revealed that Rvs167-GFP arrived at the patch after Abp1-RFP in WT cells, but upon the deletion of Pil1, Rvs167-GFP is often missing from the cortical patch (Fig. 2C). Moreover, the frequency at which endocytic sites undergo scission was significantly reduced in the mutant cells. Only 15% ($n = 30$ patches) of Rvs161-GFP and 38% ($n = 24$) of Rvs167-GFP patches in the *pil1*Δ cells showed successful endocytic internalization (Fig. 2D), suggesting that most of the endocytic sites carrying GFP-fused amphiphysin in the *pil1*Δ cells are aborted.

In light of a recent finding that *PIL1* interacts genetically with *SJL2* (Fiedler et al., 2009), we next examined the subcellular localization of the GFP-fused synaptojanins, Sjl1-, Sjl2-, and Sjl3-GFP in *pil1*Δ cells. A previous study showed that Sjl1-GFP localizes to the cell cortex and the cytoplasm (Sun et al., 2007). However, as shown in Fig. 2A, Sjl1-GFP was exclusively localized in the cytoplasm in cells lacking Pil1. Strikingly, Sjl2-GFP, an actin patch component (Stefan et al., 2005; Sun et al., 2007), was also mislocalized to the cytoplasm in *pil1*Δ cells. Finally, Sjl3-GFP localization to Trans-Golgi Network (Bensen et al., 2000; Ha et al., 2003) appears unaltered upon the loss of Pil1 (Fig. 2A).

Abp1-GFP dynamics in codeletant of PIL1 and SJL2

To examine whether Sjl2 is involved in Pil1's function on the dynamics of Abp1-GFP, we generated a haploid *pil1*Δ*sjl2*Δ double mutant through tetrad dissection. In a spotting assay, we tested whether the co-deletion of *PIL1* and *SJL2* confers a synthetic growth defect and found that the double mutant cells grew at a slower rate

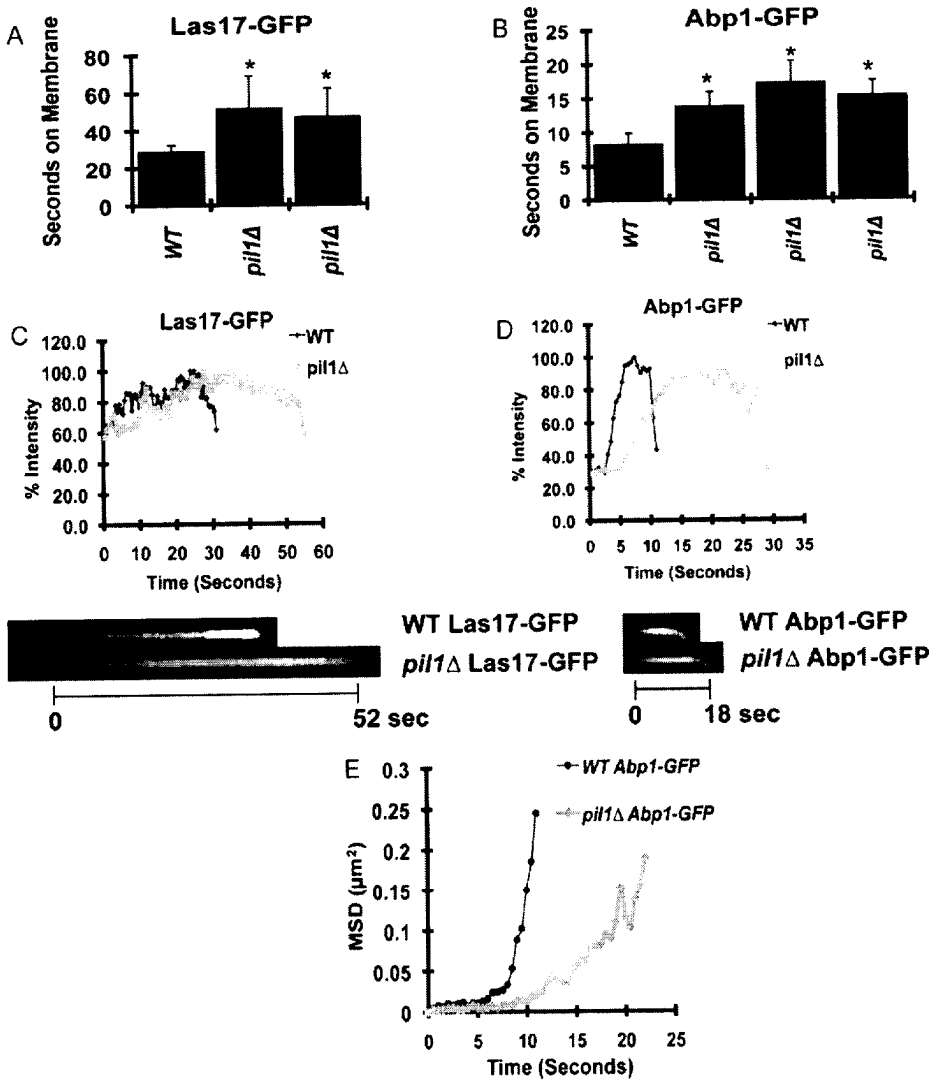

Fig. 1. Loss of Pil1 leads to extended membrane lifespan for endocytic proteins Las17-GFP and Abp1-GFP. (A) Mean lifespan of Las17-GFP on the membrane. Twenty patches were analyzed for each strain to generate the lifespan and the standard deviation. The Las17-GFP lifetime difference between WT and *pil1*Δ cells was significantly different (*$p < 0.001$). (B) Mean lifespan of Abp1-GFP on the membrane. Twenty to thirty patches were analyzed for each strain (one WT and three independently created *pil1*Δ cells) to generate the mean lifespan and the standard deviation. The Abp1-GFP lifetime difference between WT and *pil1*Δ cells was significantly different (*$p < 0.001$). (C) Quantitation of fluorescence intensity of Las17-GFP over time. The maximum fluorescence intensity of each GFP-labeled patch was normalized to 100%. Each line represents the intensity profile of one patch. Las17-GFP in *pil1*Δ cells displays a longer lifespan on the membrane. As shown by a kymographic representation, the membrane lifespan of Las17-GFP increased significantly upon the loss of Pil1. (D) Quantitation of fluorescence intensity of Abp1-GFP over time. A kymographic analysis reveals that the membrane lifespan of Abp1-GFP increased significantly upon the loss of Pil1. (E) Mean squared displacement (MSD) curves for Abp1-GFP in WT and *pil1*Δ cells. Thirty patches from each strain were analyzed from the time of patch formation until their disappearance.

at both 30 °C and 37 °C (Fig. 3A). The doubling time of the mutant (*pil1*Δ*sjl2*Δ) in YPD liquid was found to be about 2.3 h, an increase of 65% or 50 min from that of WT (1.5 h, Fig. 3B). Since it was shown by Krogan et al. (2006) that Pil1 physically interacts with Rvs161, we tested the possibility of a genetic interaction between *PIL1* and the two amphiphysins *RVS161* and *RVS167*. We observed no synthetic growth defect in the two double mutants of *pil1*Δ*rvs161*Δ and *pil1*Δ*rvs167*Δ at 30 °C, whereas both mutants showed only a slight growth defect at 37 °C (Data not shown). In order to find whether the combined deletion of *PIL1* and *SJL2*, *RVS161*, or *RVS167* might exacerbate the observed defects (extended lifetime as shown in Fig. 1) of Abp1-GFP dynamics in *pil1*Δ cells, we measured the membrane lifespan of Abp1-GFP and the scission efficiency of Abp1-GFP carrying endocytic vesicles in all double mutant strains. Surprisingly, even at the optimal temperature (30 °C), all three double mutants, *pil1*Δ*sjl2*Δ, *pil1*Δ*rvs161*Δ, and *pil1*Δ*rvs167*Δ, displayed a three- to five-fold increase in mean lifespan of Abp1-GFP on the membrane with the most extreme being *pil1*Δ*rvs161*Δ (52 s) when compared to that of WT (8.2 s) (Fig. 3C). Interestingly, the mean Abp1-GFP lifespans in the double mutant *pil1*Δ*rvs161*Δ and *pil1*Δ*rvs167*Δ strains were essentially the same as that in the single mutants, *rvs161*Δ and *rvs167*Δ cells, suggesting no additive defect is caused by the co-deletion of *PIL1* and either one of the amphiphysin proteins. In contrast, the mean membrane lifespan of Abp1-GFP in *pil1*Δ*sjl2*Δ was significantly higher than that of the single deletion mutants (*pil1*Δ and *sjl2*Δ). Furthermore, the extended membrane lifespan of Abp1-GFP in those single and double deletion mutants was found to be well correlated with the severity of endocytic scission failure (Fig. 3D) and the severity of the defect in endocytic vesicle internalization motility (Fig. 3E). Therefore, the deletion of *SJL2*, but not *RVS161* and *RVS167*, in the *pil1*Δ background led to an additional aggravation in Abp1-GFP

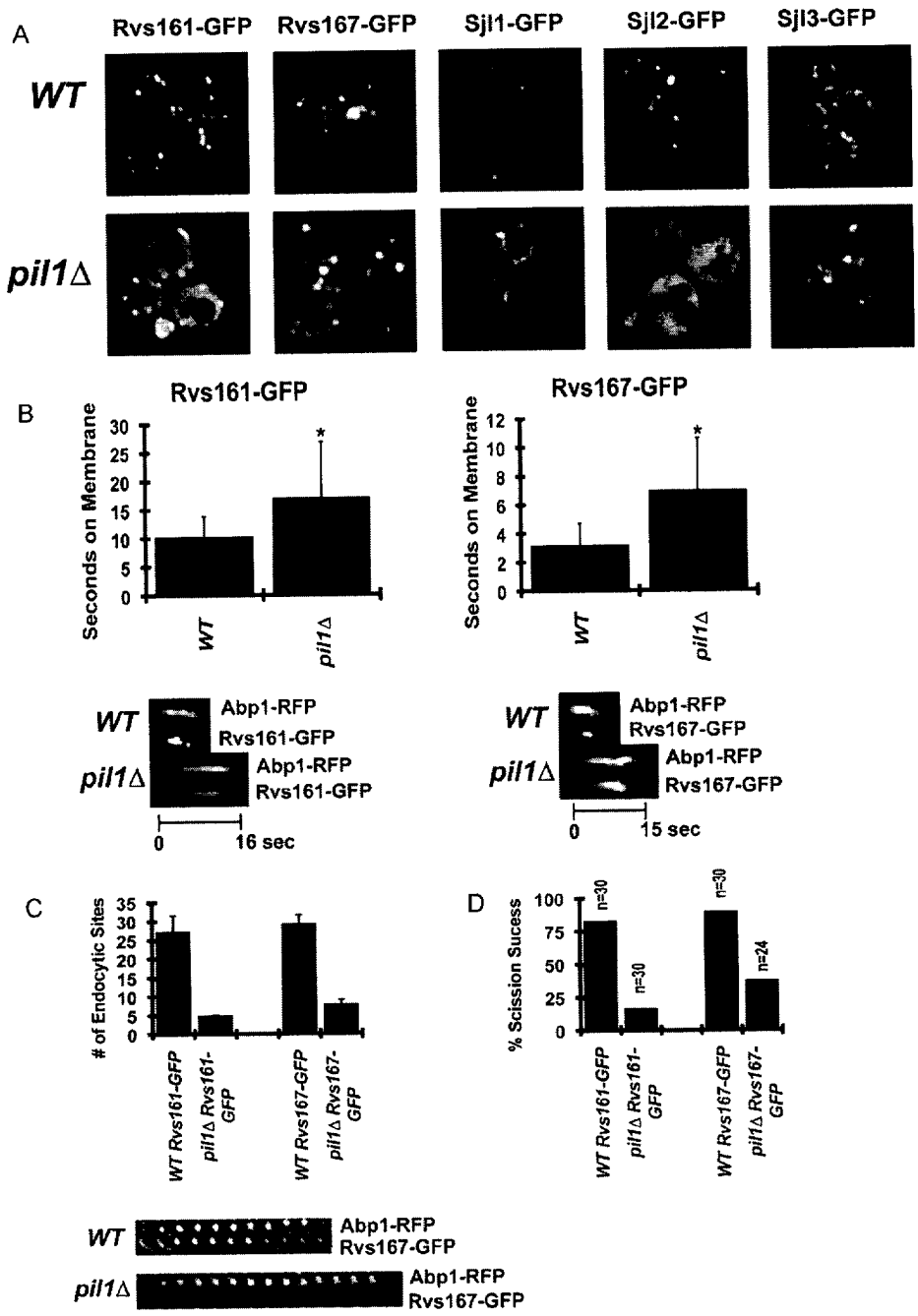

Fig. 2. The recruitment of the amphiphysins and the synaptojanins was impaired in *pil1*Δ cells. (A) The localization of several key endocytic proteins was tested in *pil1*Δ cells. WT cells show proper localization of all tested proteins to the cortical actin patch. Upon loss of Pil1, Rvs161-GFP and Rvs167-GFP are partially mislocalized, whereas Sjl1-GFP and Sjl2-GFP are completely mislocalized to the cytoplasm. (B) Mean membrane lifespan of scission proteins Rvs161-GFP and Rvs167-GFP in WT and *pil1*Δ cells. Twenty to thirty patches were analyzed to determine the mean lifespan. Upon loss of Pil1, both Rvs161-GFP and Rvs167-GFP show a significant increase in their lifespan (*$p < 0.001$). Kymographic representations show that Abp1-RFP colocalizes with Rvs161-GFP and Rvs167-GFP, where Abp1-RFP is recruited first and remains longer than either Rvs161-GFP or Rvs167-GFP. Note that the lifespan of Rvs161 and Rvs167 is extended upon the loss of Pil1. (C) Average number of endocytic sites carrying Rvs161- and Rvs167-GFP. Data was analyzed by averaging the number of the cortical GFP patches that formed in three medium-budded cells within 1 min. Both the number of endocytic sites containing Rvs161-GFP and Rvs167-GFP decreased upon the loss of Pil1. Dual imaging of Abp1-RFP and Rvs167-GFP shows that both Rvs167-GFP and Abp1-RFP are present at the same endocytic site in WT cells. However, we have often observed that Rvs167-GFP and Rvs161-GFP were missing from the endocytic patch in *pil1*Δ cells. (D) Percent scission success in WT and *PIL1*-deficient cells. Scission success was measured by counting the number of patches that showed successful internalization.

dynamics, suggesting Pil1's role in receptor-mediated endocytosis functioning with Sjl2 *in vivo*.

We next tested whether the combined deletion of *PIL1* and *SJL2* might worsen the mistargeting of the amphiphysins and synaptojanins. Interestingly, we found no phenotypic differences between *pil1*Δ and *pil1*Δ*sjl2*Δ cells except that Rvs167-GFP showed ~30% increase in lifespan in *pil1*Δ*sjl2*Δ compared to *pil1*Δ (Data not shown).

It was previously shown that the actin cytoskeleton appears disorganized in *sjl1*Δ*sjl2*Δ cells (Singer-Kruger et al., 1998), and we thus reasoned that the increase in membrane lifespan of Abp1-GFP in *pil1*Δ*sjl2*Δ cells, in which Sjl1 is mislocalized, might be due

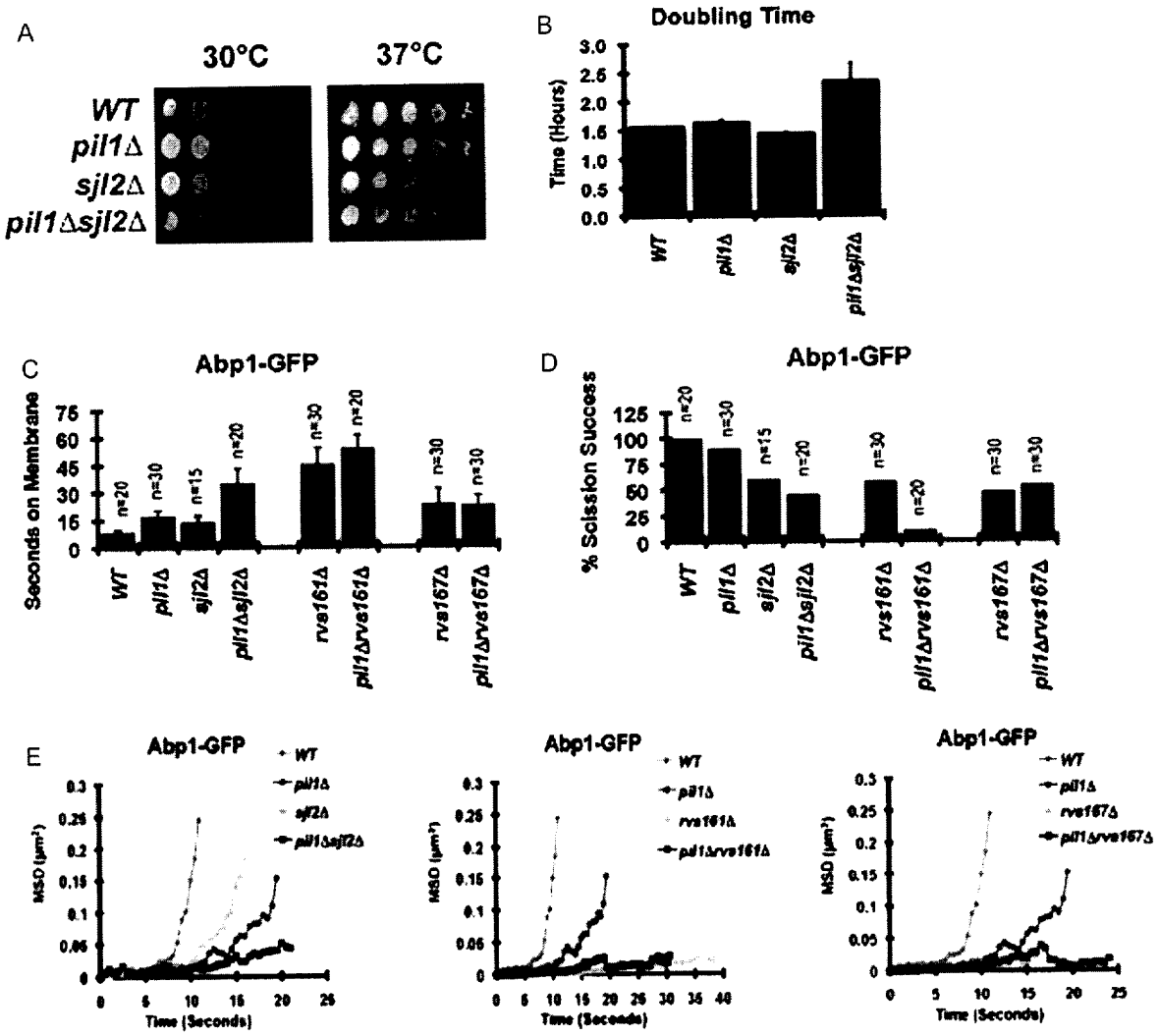

Fig. 3. The effects of codeletion of *PIL1* and *SJL2* on growth and endocytosis. (A) A growth assay on YPD plate. Cells were diluted by a factor of 5 and spotted on to YPD plates to grow overnight at 30 °C and 37 °C. *pil1Δsjl2Δ* cells grew slowly relative to single mutants. (B) Doubling time of *pil1Δsjl2Δ*. Doubling time was determined by measuring the OD at 600 nm every 90 min for 6 h. *pil1Δsjl2Δ* cells show a slight increase in the doubling time compared to WT. (C) Mean lifespan of Abp1-GFP on the membrane in various mutant cells (KKY 397, 399, 495, 528, 610, 694, 713 and 738). (D) Scission efficiency of Abp1-GFP in various mutant cells. Scission success was reduced by 50% and 90% of WT in *pil1Δsjl2Δ* and *pil1Δrvs161Δ*, respectively. (E) MSD curves for all mutant cells. Fifteen to thirty patches from each strain were analyzed from the time of patch formation until its disappearance.

to an actin defect. Indeed, our actin quantitation assay revealed that the level of actin polarization in *pil1Δsjl2Δ* cells (~20%) was much lower, compared to 82%, 83%, and 64% in WT, *pil1Δ*, *sjl2Δ* cells, respectively (Fig. 4A). Similarly, most of *pil1Δsjl2Δ* cells (95%) lack detectable intact actin cables (Fig. 4A). Noteworthy, the cortical fluorescence intensity of actin patches in *pil1Δsjl2Δ* cells increased significantly (~35%) (Fig. 4B), indicating more F-actin associated with the cortical endocytic sites. However, the total actin levels were constant across all cells (WT, *pil1Δ*, *sjl2Δ*, and *pil1Δsjl2Δ*), manifested in Western blot analysis (Fig. 4C).

Discussion

Over the past several years, rapid advances in eisosome research regarding the molecular requirements of eisosome organization have not only greatly contributed to our knowledge of the structure and function of the plasma membrane but also raised new questions concerning the role of the eisosome in endocytosis. The eisosome was originally thought to be involved in endocytosis based on the observation that the distribution of the eisosome marker Pil1 coincides partially with the membrane-phase endocytosis marker FM4-64 (Walther et al., 2006). Furthermore, it appears that the extent of spatial overlapping between the eisosome and FM4-64 increases as aberrant eisosome aggregates formed by the loss of Pil1, indicating that eisosomes serve as the static marker for endocytic sites (Walther et al., 2006). The authors also demonstrated the implication of Pil1 in receptor mediated endocytosis by revealing that the rate of Ste3 degradation in the vacuole in *pil1Δ* cells decreased significantly when compared to that in WT cells. Additionally, it was found that the frequency at which furrow-like membrane invaginations occur in cells deficient of Pil1 was as low as 20% of WT cells (Stradalova et al., 2009), consistent with the data provided by Walther et al. (2006) that *pil1Δ* cells display only a few eisosome remnants that contained two fiduciary markers for receptor mediated endocytosis, Abp1 and Sla1. Therefore, the association

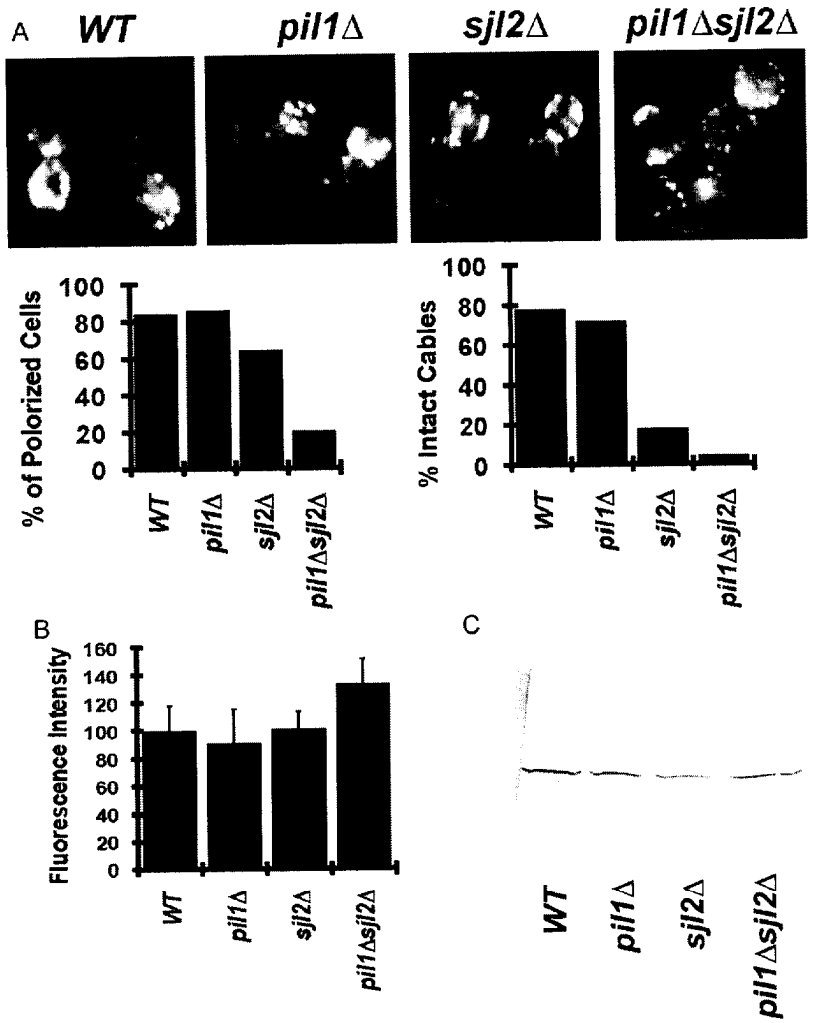

Fig. 4. Loss of Pil1 and Sjl2 leads to a severe actin disruption. (A) Representative images of the actin organization by FITC-phalloidin staining. The extent of actin polarization and the percent of cells with intact actin cables were analyzed. *SJL2*-deficient cells showed normal levels in actin patch polarization but a severe loss of actin cables, while *pil1Δsjl2Δ* cells displayed a dramatic loss of both actin polarization and intact actin cables. (B) Quantification of F-actin levels at the cortical endocytic sites in the mutant cells. Fluorescence intensity of FITC-labeled actin patches was measured. The mean fluorescence intensity of WT actin patches was normalized to 100%. (C) Western blot showing the levels of total actin in various mutants (KKY 194, 197, 421 and 490).

of the rest of the actin-based endocytic machinery to the aberrant structure is highly likely.

Our results in this study provide several lines of evidence pointing consistently to the conclusion that Pil1 plays important indirect roles in recepter mediated endocytosis through the recuirtment of certain enodcytic proteins: (1) it appears that intact eisosome structures are essentially required for the proper recruitment of the two synaptojanins Sjl1 and Sjl2 to endocytic sites (Fig. 2A); (2) the lifespans of actin binding proteins at endocytic sites including Abp1 and Las17 increased markedly upon the loss of Pil1 (Fig. 1); (3) loss of Pil1 resulted in fewer cortical endocytic patches carrying Rvs161- and Rvs167-GFP (Fig. 2).

However, it seems clear that endocytic events (receptor mediated endocytosis) are excluded from the eisosome and membrane compartment of Can1 (MCC). First, it is because of the observation that Sur7, a MCC component, does not localize to the classical endocytic sites carrying Rvs161 and Ede1 (Grossmann et al., 2008). Second, Brach et al. (2011) consistently reported that Pil1-mCherry puncta are not spatially overlapping with Abp1-GFP. Rather, Brach et al. (2011) found that endocytic sites are restricted to another membrane compartment carrying Pma1 (MCP) that surrounds the MCC puncta.

An optimal membrane level of PIP_2 is maintained primarily by several phosphoinositide kinases and phosphatases (Boronenkov and Anderson, 1995; Homma et al., 1998; Hughes et al., 2000; Strahl and Thorner, 2007), and the lack of or imbalance of those enzymes results in altered PIP_2 levels and endocytic defects (Cremona et al., 1999; Di Paolo et al., 2004; Singer-Kruger et al., 1998). For example, synaptojanin-deficient cells, in which levels of membrane PIP_2 increase (Stefan et al., 2002), displayed a significant defect in liquid phase endocytosis on the basis of the observation that the endocytic transit of FM4-64 was in part blocked (Stefan et al., 2005). In light of our finding that both Sjl1 and Sjl2 are mistargeted to the cytoplasm in *PIL1*-deficient cells (Fig. 2A), we reasoned that the membrane PIP_2 levels in *pil1Δ* cells should increase. Interestingly, *pil1Δ* cells expressing a PIP_2-binding GFP-2XPH plasmid appeared to display an increased level of membrane GFP fluorescence than WT (Data not shown). However, considering that the expression level of PH-GFP on a plasmid varies from cell to cell, one needs a biochemical methods such as labeling of phosphoinositols with H^3 in conjunc-

tion with HPLC to quantitate precise levels of PIP_2, as previously described (Stefan et al., 2002). What might be the possible cause for the mislocalization of the synaptojanins? It has previously been shown that Abp1 is essential for the proper recruitment of Sjl2 to the cortical actin patches (Fazi et al., 2002; Stefan et al., 2005). However, we rule out the possibility that Abp1 serves as a primary factor for the recruitment of the synaptojanins based on the observation that loss of Pil1 does not affect the localization of Abp1-GFP (Fig. 1). It was found that Bsp1, an actin patch component, physically interacts with the N-terminal Sac1 domain of Sjl2, and was proposed that Bsp1 is an adaptor that links Sjl2 to actin patches (Wicky et al., 2003). However, we observed that Bsp1-GFP is properly targeted to the actin patch upon the loss of Pil1, and therefore other factors are important for the recruitment of Sjl2 to the membrane. Importantly, the observations of partial mislocalization of Sjl2 in *rvs167Δ* and *rvs161Δ* cells (Stefan et al., 2005) (our unpublished results) led us to propose that the amphiphysins Rvs161 and Rvs167 play a role in the cortical recruitment of Sjl2. Furthermore, it appears that the deletion of *PIL1* causes fewer Rvs161- and Rvs167-GFP molecules to be recruited to the membrane (Fig. 2A and C). It is therefore possible that an optimal amount of amphiphysin complex (Rvs161-Rvs167) at the cortical endocytic sites is required for proper recruitment of Sjl2. Given that a disruption in sphingolipid synthesis affects the subcellular localization of the amphiphysins (Balguerie et al., 2002; Youn et al., 2010), our explanation for the possible grounds of the partial mislocalization of the amphiphysins in *pil1Δ* cells is that levels of complex sphingolipids might be significantly altered by deletion of Pil1. It has been shown that the lipid binding Slm proteins (Slm1 and Slm2) take part in regulating sphingolipid levels, and inactivation of those proteins was found to be a leading cause for defects in sphingolipid biosynthesis (Dickson, 2008; Tabuchi et al., 2006). Furthermore, our recent observation of mislocalization of Slm1 and Slm2 to the cytoplasm in the absence of Pil1 (Kamble et al., 2011) suggests the possibility of sphingolipid disruption in *pil1Δ* cells, thereby mimicking the effect of inactivation of Slm proteins.

Acknowledgments

We thank Dr. Scott Emr for providing the strain *sjl2Δ*. We thank members of the Kim lab for thoughtful discussion and insight. This work was supported by a National Scientific Foundation Grant 0923024 (to K. Kim) and by thesis funding from Missouri State University (to E. Murphy).

Appendix A. Supplementary data

Supplementary data associated with this article can be found, in the online version, at doi:10.1016/j.ejcb.2011.06.006.

References

Balguerie, A., Bagnat, M., Bonneu, M., Aigle, M., Breton, A.M., 2002. Rvs161p and sphingolipids are required for actin repolarization following salt stress. Eukaryot. Cell 1, 1021–1031.

Bensen, E.S., Costaguta, G., Payne, G.S., 2000. Synthetic genetic interactions with temperature-sensitive clathrin in *Saccharomyces cerevisiae*. Roles for synaptojanin-like Inp53p and dynamin-related Vps1p in clathrin-dependent protein sorting at the trans-Golgi network. Genetics 154, 83–97.

Boronenkov, I.V., Anderson, R.A., 1995. The sequence of phosphatidylinositol-4-phosphate 5-kinase defines a novel family of lipid kinases. J. Biol. Chem. 270, 2881–2884.

Brach, T., Specht, T., Kaksonen, M., 2011. Reassessment of the role of plasma membrane domains in the regulation of vesicular traffic in yeast. J. Cell Sci. 124, 328–337.

Carlsson, A.E., Shah, A.D., Elking, D., Karpova, T.S., Cooper, J.A., 2002. Quantitative analysis of actin patch movement in yeast. Biophys. J. 82, 2333–2343.

Cremona, O., Di Paolo, G., Wenk, M.R., Luthi, A., Kim, W.T., Takei, K., Daniell, L., Nemoto, Y., Shears, S.B., Flavell, R.A., et al., 1999. Essential role of phosphoinositide metabolism in synaptic vesicle recycling. Cell 99, 179–188.

Di Paolo, G., Moskowitz, H.S., Gipson, K., Wenk, M.R., Voronov, S., Obayashi, M., Flavell, R., Fitzsimonds, R.M., Ryan, T.A., De Camilli, P., 2004. Impaired PtdIns(4,5)P2 synthesis in nerve terminals produces defects in synaptic vesicle trafficking. Nature 431, 415–422.

Dickson, R.C., 2008. Thematic review series: sphingolipids. New insights into sphingolipid metabolism and function in budding yeast. J. Lipid Res. 49, 909–921.

Fazi, B., Cope, M.J., Douangamath, A., Ferracuti, S., Schirwitz, K., Zucconi, A., Drubin, D.G., Wilmanns, M., Cesareni, G., Castagnoli, L., 2002. Unusual binding properties of the SH3 domain of the yeast actin-binding protein Abp1: structural and functional analysis. J. Biol. Chem. 277, 5290–5298.

Fiedler, D., Braberg, H., Mehta, M., Chechik, G., Cagney, G., Mukherjee, P., Silva, A.C., Shales, M., Collins, S.R., van Wageningen, S., et al., 2009. Functional organization of the *S. cerevisiae* phosphorylation network. Cell 136, 952–963.

Frohlich, F., Moreira, K., Aguilar, P.S., Hubner, N.C., Mann, M., Walter, P., Walther, T.C., 2009. A genome-wide screen for genes affecting eisosomes reveals Nce102 function in sphingolipid signaling. J. Cell Biol. 185, 1227–1242.

Galletta, B.J., Cooper, J.A., 2009. Actin and endocytosis: mechanisms and phylogeny. Curr. Opin. Cell Biol. 21, 20–27.

Grossmann, G., Malinsky, J., Stahlschmidt, W., Loibl, M., Weig-Meckl, I., Frommer, W.B., Opekarova, M., Tanner, W., 2008. Plasma membrane microdomains regulate turnover of transport proteins in yeast. J. Cell Biol. 183, 1075–1088.

Grossmann, G., Opekarova, M., Malinsky, J., Weig-Meckl, I., Tanner, W., 2007. Membrane potential governs lateral segregation of plasma membrane proteins and lipids in yeast. EMBO J. 26, 1–8.

Ha, S.A., Torabinejad, J., DeWald, D.B., Wenk, M.R., Lucast, L., De Camilli, P., Newitt, R.A., Aebersold, R., Nothwehr, S.F., 2003. The synaptojanin-like protein Inp53/Sjl3 functions with clathrin in a yeast TGN-to-endosome pathway distinct from the GGA protein-dependent pathway. Mol. Biol. Cell 14, 1319–1333.

Homma, K., Terui, S., Minemura, M., Qadota, H., Anraku, Y., Kanaho, Y., Ohya, Y., 1998. Phosphatidylinositol-4-phosphate 5-kinase localized on the plasma membrane is essential for yeast cell morphogenesis. J. Biol. Chem. 273, 15779–15786.

Hughes, W.E., Cooke, F.T., Parker, P.J., 2000. Sac phosphatase domain proteins. Biochem. J. 350 (Pt 2), 337–352.

Idrissi, F.Z., Grotsch, H., Fernandez-Golbano, I.M., Presciatto-Baschong, C., Riezman, H., Geli, M.I., 2008. Distinct acto/myosin-I structures associate with endocytic profiles at the plasma membrane. J. Cell Biol. 180, 1219–1232.

Jonsdottir, G.A., Li, R., 2004. Dynamics of yeast Myosin I: evidence for a possible role in scission of endocytic vesicles. Curr. Biol. 14, 1604–1609.

Kaksonen, M., Sun, Y., Drubin, D.G., 2003. A pathway for association of receptors, adaptors, and actin during endocytic internalization. Cell 115, 475–487.

Kaksonen, M., Toret, C.P., Drubin, D.G., 2005. A modular design for the clathrin- and actin-mediated endocytosis machinery. Cell 123, 305–320.

Kamble, C., Jain, S., Murphy, E., Kim, K., 2011. Requirements of Slm proteins for proper eisosome organization, endocytic trafficking and recycling in the yeast *Saccharomyces cerevisiae*. J. Biosci. 36, 79–96.

Kim, K., Galletta, B.J., Schmidt, K.O., Chang, F.S., Blumer, K.J., Cooper, J.A., 2006. Actin-based motility during endocytosis in budding yeast. Mol. Biol. Cell 17, 1354–1363.

Krogan, N.J., Cagney, G., Yu, H., Zhong, G., Guo, X., Ignatchenko, A., Li, J., Pu, S., Datta, N., Tikuisis, A.P., et al., 2006. Global landscape of protein complexes in the yeast *Saccharomyces cerevisiae*. Nature 440, 637–643.

Liu, J., Sun, Y., Drubin, D.G., Oster, G.F., 2009. The mechanochemistry of endocytosis. PLoS Biol. 7, e1000204.

Longtine, M.S., McKenzie 3rd, A., Demarini, D.J., Shah, N.G., Wach, A., Brachat, A., Philippsen, P., Pringle, J.R., 1998. Additional modules for versatile and economical PCR-based gene deletion and modification in *Saccharomyces cerevisiae*. Yeast (Chichester, England) 14, 953–961.

Merrifield, C.J., Qualmann, B., Kessels, M.M., Almers, W., 2004. Neural Wiskott Aldrich Syndrome Protein (N-WASP) and the Arp2/3 complex are recruited to sites of clathrin-mediated endocytosis in cultured fibroblasts. Eur. J. Cell Biol. 83, 13–18.

Moreira, K.E., Walther, T.C., Aguilar, P.S., Walter, P., 2009. Pil1 controls eisosome biogenesis. Mol. Biol. Cell 20, 809–818.

Nannapaneni, S., Wang, D., Jain, S., Schroeder, B., Highfill, C., Reustle, L., Pittsley, D., Maysent, A., Moulder, S., McDowell, R., et al., 2010. The yeast dynamin-like protein Vps1:vps1 mutations perturb the internalization and the motility of endocytic vesicles and endosomes via disorganization of the actin cytoskeleton. Eur. J. Cell Biol. 89, 499–508.

Newpher, T.M., Smith, R.P., Lemmon, V., Lemmon, S.K., 2005. In vivo dynamics of clathrin and its adaptor-dependent recruitment to the actin-based endocytic machinery in yeast. Dev. Cell 9, 87–98.

Singer-Kruger, B., Nemoto, Y., Daniell, L., Ferro-Novick, S., De Camilli, P., 1998. Synaptojanin family members are implicated in endocytic membrane traffic in yeast. J. Cell Sci. 111 (Pt 22), 3347–3356.

Stefan, C.J., Audhya, A., Emr, S.D., 2002. The yeast synaptojanin-like proteins control the cellular distribution of phosphatidylinositol (4,5)-bisphosphate. Mol. Biol. Cell 13, 542–557.

Stefan, C.J., Padilla, S.M., Audhya, A., Emr, S.D., 2005. The phosphoinositide phosphatase Sjl2 is recruited to cortical actin patches in the control of vesicle formation and fission during endocytosis. Mol. Cell. Biol. 25, 2910–2923.

Stradalova, V., Stahlschmidt, W., Grossmann, G., Blazikova, M., Rachel, R., Tanner, W., Malinsky, J., 2009. Furrow-like invaginations of the yeast plasma membrane correspond to membrane compartment of Can1. J. Cell Sci. 122, 2887–2894.

Strahl, T., Thorner, J., 2007. Synthesis and function of membrane phosphoinositides in budding yeast, *Saccharomyces cerevisiae*. Biochim. Biophys. Acta 1771, 353–404.

Sun, Y., Carroll, S., Kaksonen, M., Toshima, J.Y., Drubin, D.G., 2007. PtdIns(4,5)P2 turnover is required for multiple stages during clathrin- and actin-dependent endocytic internalization. J. Cell Biol. 177, 355–367.

Tabuchi, M., Audhya, A., Parsons, A.B., Boone, C., Emr, S.D., 2006. The phosphatidylinositol 4,5-biphosphate and TORC2 binding proteins Slm1 and Slm2 function in sphingolipid regulation. Mol. Cell. Biol. 26, 5861–5875.

Toret, C.P, Lee, L., Sekiya-Kawasaki, M., Drubin, D.G., 2008. Multiple pathways regulate endocytic coat disassembly in *Saccharomyces cerevisiae* for optimal downstream trafficking. Traffic (Copenhagen, Denmark) 9, 848–859.

Walther, T.C., Aguilar, P.S., Frohlich, F., Chu, F., Moreira, K., Burlingame, A.L., Walter, P., 2007. Pkh-kinases control eisosome assembly and organization. EMBO J. 26, 4946–4955.

Walther, T.C., Brickner, J.H., Aguilar, P.S., Bernales, S., Pantoja, C., Walter, P., 2006. Eisosomes mark static sites of endocytosis. Nature 439, 998–1003.

Wicky, S., Frischmuth, S., Singer-Kruger, B., 2003. Bsp1p/Ypr171p is an adapter that directly links some synaptojanin family members to the cortical actin cytoskeleton in yeast. FEBS Lett. 537, 35–41.

Youn, J.Y., Friesen, H., Kishimoto, T., Henne, W.M., Kurat, C.F., Ye, W., Ceccarelli, D.F., Sicheri, F., Kohlwein, S.D., McMahon, H.T., et al., 2010. Dissecting BAR domain function in the yeast Amphiphysins Rvs161 and Rvs167 during endocytosis. Mol. Biol. Cell 21, 3054–3069.

Zhang, X., Lester, R.L., Dickson, R.C., 2004. Pil1p and Lsp1p negatively regulate the 3-phosphoinositide-dependent protein kinase-like kinase Pkh1p and downstream signaling pathways Pkc1p and Ypk1p. J. Biol. Chem. 279, 22030–22038.